Quantitative Spectral Data Acquisition and Analysis with Modular Smartphone Assemblies

by

Michael Robert Harradon

S.B., MIT, 2013

Submitted to the Department of Electrical Engineering and Computer Science

in Partial Fulfillment of the Requirements for the Degree of

Master of Engineering in Electrical Engineering and Computer Science

at the

MASSACHUSETTS INSTITUTE OF TECHNOLOGY

September 2014

Signature redacted

Author .....
Department of Electrical Engineering and Computer Science
September 8, 2014

Certified by..... Signature redacted .....
Prof. Ramesh Raskar
Associate Professor of Media Arts and Sciences
Thesis Supervisor

Certified by.. Signature redacted .....
Dr. Zigurts Majumdar
Booz Allen Hamilton
Signature redacted
Thesis Supervisor

Accepted by . .....
Prof. Albert R. Meyer
Chairman, Masters of Engineering Thesis Committee

Quantitative Spectral Data Acquisition and Analysis with Modular Smartphone Assemblies

by

Michael Robert Harradon

Submitted to the Department of Electrical Engineering and Computer Science
on September 8, 2014, in partial fulfillment of the
requirements for the degree of
Master of Engineering in Electrical Engineering and Computer Science

Abstract

A low-cost cell phone spectrometer using the image sensor in the cell phone camera is developed and analyzed. The spectrometer design is optimized for sensitivity and spectral resolution. Calibration techniques are developed to enable robust data collection across different phone models with minimal equipment. Novel algorithms for robust calibration with minimal equipment are described and implemented. The spectrometer is then characterized for use in colorimetric systems. Finally, the cell phone spectrometer is used in a forensic application for dating blood spots based on time-dependent oxidation-induced spectral changes.

Thesis Supervisor: Prof. Ramesh Raskar
Title: Associate Professor of Media Arts and Sciences

Thesis Supervisor: Dr. Zigurts Majumdar
Title: Booz Allen Hamilton

Acknowledgments

Thanks to my family and friends who have supported me as I worked on my thesis project. A special thanks to everyone at Booz Allen Hamilton for all of their assistance and support in the development of my thesis project as part of my VI-A program, including Kristen O'Connor, Gino Serpa, Paul D'Angio, Matt Frazier and Sheila Barber, and especially my advisors Ziggy Majumdar and Rich Lepkowicz. Their mentorship while working in DC was invaluable. An additional thanks to Professor Daniele Podini and his researchers Michelle Mendonca and Nichole Sutton at George Washington University's forensics lab, as without their hard work and assistance the lab studies could have never been completed.

THIS PAGE INTENTIONALLY LEFT MOSTLY BLANK

Contents

Chapter 1

Introduction

1.1 Spectroscopy

Spectroscopy is a common technique for analyzing materials and chemicals. In the case of visible spectroscopy, to which this thesis pertains, a substance is illuminated with a broad specta light source i.e. white light. A substance's absorption in general varies with wavelength, and as a result the reflected light has a different intensity distribution than the incident light. For the vast majority of substances this can be modeled as a linear absorption as a function of frequency. By measuring the reflected light and dividing it by the known illumination spectra it is possible to deduce a reflectance spectra. Alternately, in the case of a spectrophotometer, a transmission spectra can be identified. In many cases the illumination spectra is unknown, however - in this case one often first measures an object of known, broad spectra and uses the measurement to deduce the illumination spectra for future measurements. Here M denotes measurements, I denotes illumination and R denotes reflectance spectra.

$$M_{measurement}(\lambda) = R_{sample}(\lambda) \cdot I_{illumination}(\lambda) \tag{1.1}$$

$$I_{illumination}(\lambda) = M_{calibration}(\lambda)/R_{known}(\lambda) \tag{1.2}$$

Spectroscopy in the visible range has numerous applications ranging including biology [5], chemistry [7], forensics [2] and medicine [1]. Thanks to the recent prolifereration of smart phones many people carry cameras connected directly to an easily programmable computer. Developing a capacity for these phones to take some subset of useful spectroscopic measurements could lower the barrier of entry to a wide variety of measurements.

1.2 Mobile Spectoscopy

Enabling spectroscopy on mobile platforms has been investigated by a number of researchers [8] [6] [4]. These projects have generally focused on bare minimum platforms for ultra-low-cost applications. The simplest designs consist of CDs used as diffractive elements and a slit placed at a distance as the only collimation system. Here we consider a slightly more expensive ($5 at scale) module with enhanced performance capabilities using commercial but still low-cost optical components. In addition, we consider the steps required to make the quantitative measurements. In order to use a cell phone camera as a rigorous, performance spectrometer there are a number of aspects that must be considered:

1. An optical model of the cell phone camera must be constructed.
2. A parametric model of a spectrometer must be designed.
3. The spectrometer model must be optimized over its parameters.
4. The spectrometer must be built, tested and characterized.

These components form the bulk of this thesis.

Chapter 2

Spectrometer Design and Analysis

2.1 Analysis and Optimization of Generalized Spectrometer

2.1.1 Overview

A simple generalized spectrometer could be considered to be made of 5 main components. First, there is an aperture, often taking the form of a slit. Next, there is a collimation optic that forms light from the aperture into a beam with minimal angular divergence. The beam then passes through a third component, the dispersive optic. The dispersive optic, often a prism or diffraction grating, emits light at different angles corresponding to wavelength. A fourth component, an imaging optic, focuses light traveling at different angles onto different spots corresponding to angle (and thus wavelength). Finally, a fifth component, an image sensor, detects light at the different points and relays it to processing electronics. Each pixel in the image is then mapped to a wavelength band either by optical analysis of the system or calibration procedure.

2.1.2 Aperture and Collimating Optics

Of primary interest is the design of the first stages of the optical system. In order to collimate incident light it must first pass through a limiting aperture and then though a lens placed one focal length away. We'll consider a slit of width d followed by a lens with focal length f_1 and diameter D_1. Basic geometric optics states that the full width of the angular deviation of the beam after collimation can be approximated by d/f_1 for small values. One can relate the system spectral resolution for a sufficiently linear dispersive optic to the angular deviation of incident light to the first order with the following equation where θ_o denotes output angle from the dispersive optic and θ_i denotes input angle:

$$\frac{\partial \theta_o}{\partial \theta_i}\delta\theta_i = \frac{\partial \theta_o}{\partial \lambda}\delta\lambda = \delta\theta_o \tag{2.1}$$

By solving for $\delta\lambda$ in terms of $\delta\theta_i$ we can find how the degree of collimation determines the spectral resolution (assuming infinitesimal pixel size on the image sensor).

$$\delta\lambda = \left(\frac{\partial \theta_o}{\partial \theta_i}\right)\left(\frac{\partial \theta_o}{\partial \lambda}\right)^{-1}\left(\frac{d}{f_1}\right) \tag{2.2}$$

For an arbitrary input light source one would expect the amount of total light transmitted to be proportional to the slit width d. We'll write that proportionality constant as k, such that $P_{in} = kd$. We can then construct a slit-independent figure-of-merit as such:

$$\frac{P_{in}}{\delta\lambda} = kf_1\left(\frac{\partial \theta_o}{\partial \theta_i}\right)^{-1}\left(\frac{\partial \theta_o}{\partial \lambda}\right) \tag{2.3}$$

This equation demonstrates the inherent tradeoff between spectrometer sensitivity and spectral resolution. Our goal is to maximize its value. Increasing the focal length of the collimating optic would be the most straightforward path, except doing so increases the size of the device as well as the size of the imaging system optics. Given that our goal is portable spectroscopy, this is often significantly limited by form factor. What remains are the two partial derivatives defined by the dispersing optic, which we will now consider in depth.

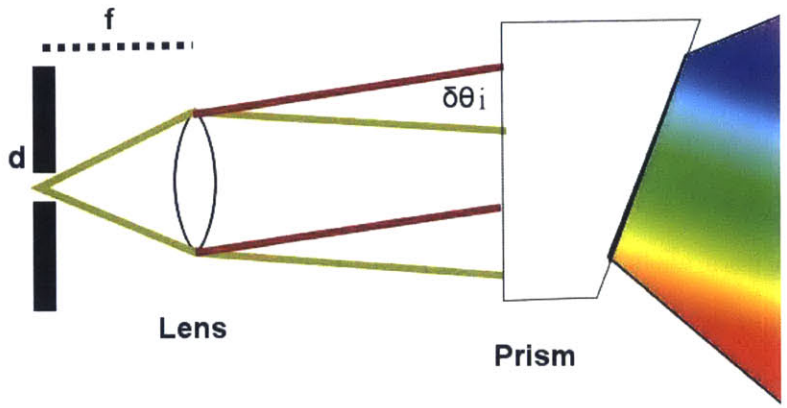

Figure 2-1: A schematic of a simple spectrometer design

2.1.3 Dispersing Optics

The most intuitive is the linear dispersion of the optic, given by $\frac{\partial \theta_o}{\partial \lambda}$. This term is fixed by the the type and orientation of the optic, and it determines the angular width of the emitted spectra. Simply put, this term sets the width of the emitted "rainbow" on the sensor. Since the "rainbow" is only sampled on a finite grid of pixels, increasing this term increases the system's spectral resolution. For the first order of a diffraction grating at direct incidence and for large periodicity $d >> \lambda$ the term is given simply as follows:

$$\frac{\partial \theta_o}{\partial \lambda} = \frac{1}{d} \tag{2.4}$$

The other term, $\left(\frac{\partial \theta_o}{\partial \theta_i}\right)^{-1}$, represents the optic's sensitivity to input angle. If one considers an ideal monochromatic input light source one would observe the peak having a finite width as the collimating optic still results in an output beam with finite angular divergence which is propagated through the dispersing optic according to this term. For the diffraction grating at small angles it is given simply as:

$$\frac{\partial \theta_o}{\partial \theta_i} = -1 \tag{2.5}$$

2.1.4 Camera Considerations

In a typical spectrometer one would normally focus light onto a monochromatic wide-response strip imager such as a bare CMOS sensor. One of the primary differences here is that our image sensor has a bayer mask on it. The bayer mask serves to enable red, green and blue channel measurements. These channels act as selective absorbers with 3 different gaussian-like transmission curves. For our purposes we can generally consider them to function as three independent spectrometers operating over 3 different bands. Simply summing them prematurely would make it much more difficult to consider the impact of sensor nonlinearity, as we will later. For final display after nonlinear correction we add the channels together to get an overall luminosity curve. As long as the response is linear it doesn't matter what the shape of the channel response is, as it will be canceled out when the measured sample spectra is divided by white.

2.2 Device Outline

The first prototype cell phone spectrometer was a cell phone case 3D printed in black plastic. Optical fibers pipe light from the phone flash to an enclosed compartment at the bottom. A second set of optical fibers carry light reflected off the sample to an optical compartment and serve as a spatially limiting "slit". A low-cost lens is placed one focal length away from the slit in order to collimate the light. A holographic diffraction grating then refracts and disperses the incident beam into a prism that reflects the light into the camera aperture. As we model the camera as being focused to infinity each wavelength is ideally focused onto a single point.

This achieved successful measurements, but intensity performance was lackluster. This was largely due to the small size of the fiber and the small fraction of incident energy transmitted into the first order. In order to improve performance a second prototype was created. The optical path was shifted to directly in front of the camera, while the diffracton grating was replace with an off the shelf spectroscope

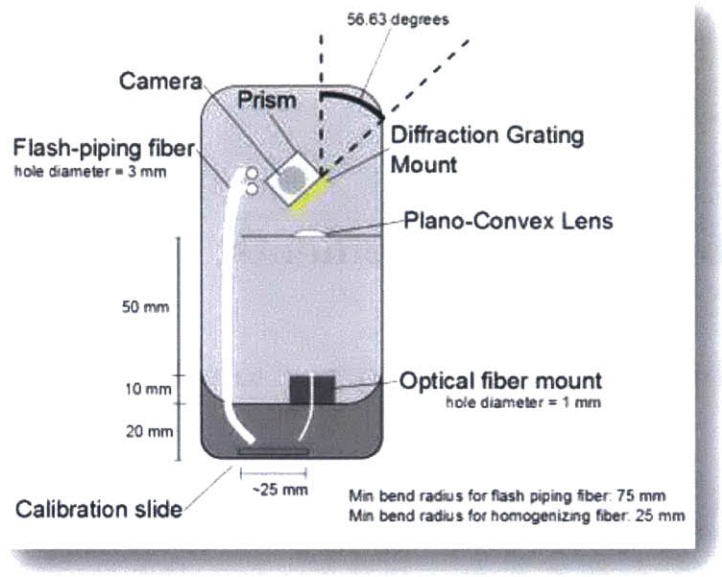

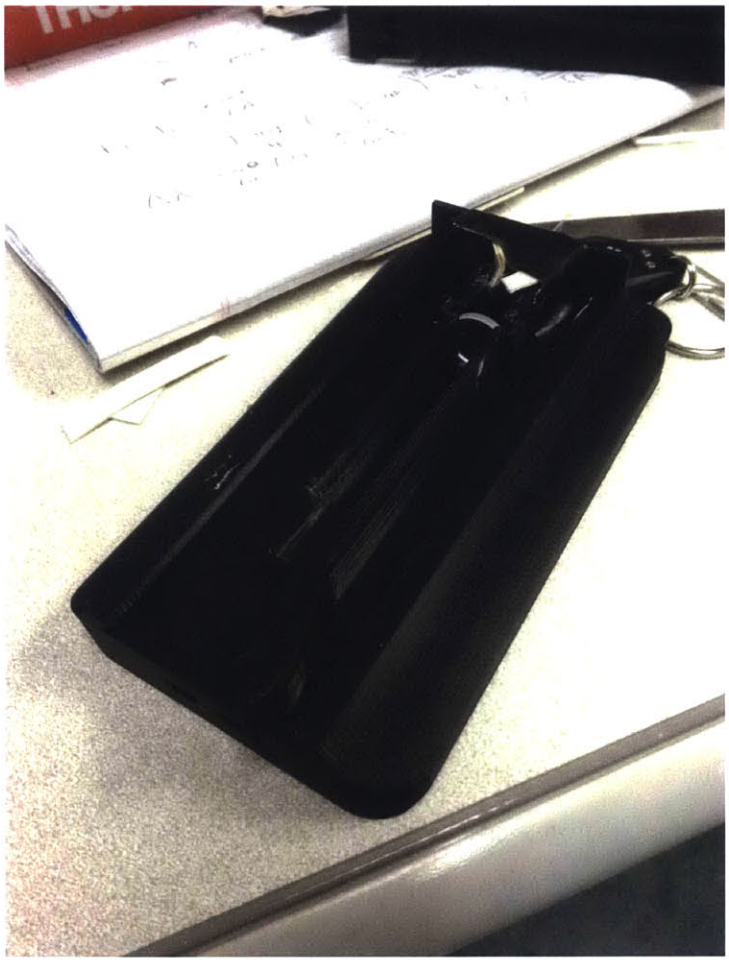

Figure 2-2: The first spectrometer prototype

containing injection molded lenses and a grism, a grated prism with greatly increased (albeit less linear) dispersion. This resulted in significantly improved performance.

2.3 Calibration Requirements

2.3.1 Nonlinear Response Correction Algorithms

As stated in the introduction, when taking a spectroscopic measurement the typical procedure is to measure an object with a known, ideally flat, response and then measure the object of interest. One then removes the effects of variation in the illumination source by simple division:

$$M_{object}(\lambda) = R_{object}(\lambda)I_{light}(\lambda) \tag{2.6}$$

$$M_{calibration}(\lambda) = R_{known}(\lambda)I_{light}(\lambda) \tag{2.7}$$

$$R_{object}(\lambda) = \frac{M_{object}(\lambda)}{M_{calibration}(\lambda)}R_{known}(\lambda) \tag{2.8}$$

This is not possible in general, however, if the measurement system exhibits a nonlinear response in intensity. Consider a measurement M taken of spectra I affected by a nonlinear response function f:

$$M_{object}(\lambda) = f(R_{object}(\lambda)I_{light}(\lambda)) \tag{2.9}$$

$$M_{calibration}(\lambda) = f(R_{known}(\lambda)I_{light}(\lambda)) \tag{2.10}$$

Simple division here is not capable of recovering the object spectra. If we can identify the nonlinear response of the sensor, however, we can reconstruct the intensity by inverting the response function:

$$R_{object}(\lambda) = \frac{f^{-1}(M_{object}(\lambda))}{f^{-1}(M_{calibration}(\lambda))}R_{known}(\lambda) \tag{2.11}$$

Figure 2-3: The second spectrometer prototype using a grism assembly

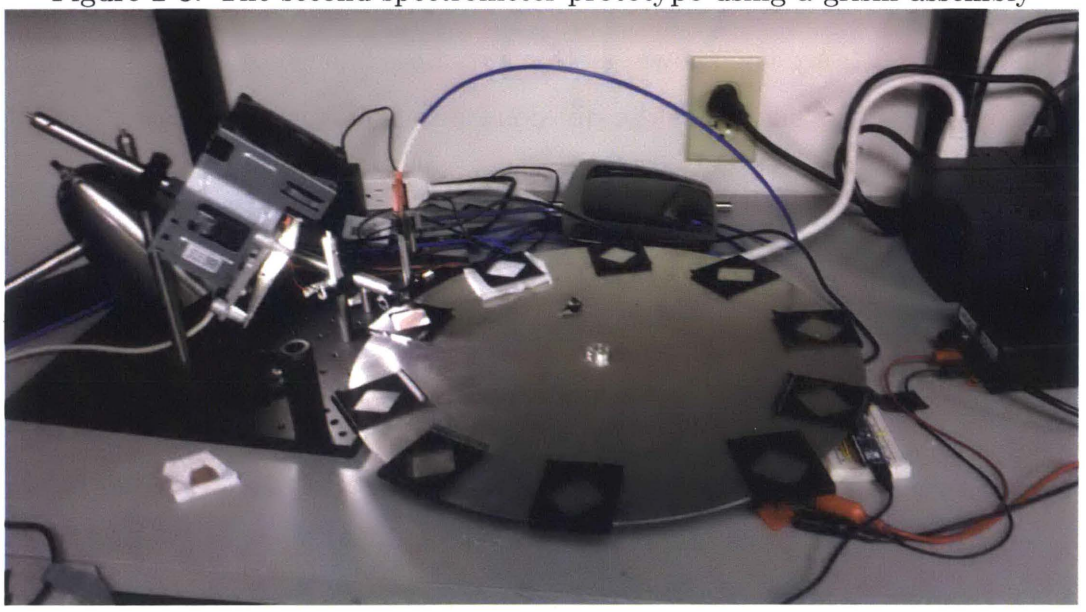

Figure 2-4: Experimental setup for measuring blood samples with phone and ocean optics standard spectrometer

Our goal is then to construct a calibration procedure that would allow recovering the intensity function. One common method for calibrating spectrometers is to use a series of known broad spectral sources, such as a calibrated lamp and attenuator. These lamps can be expensive, however, and make calibration much less accessible. It's possible, however, to deduce the relative nonlinear response of the system by simply measuring two samples of known response spectra, assuming they sufficiently cover the full dynamic range of the sensor under the used illumination. Consider measuring two objects of known spectra (argument λ assumed):

$$M_1 = f(IR_1) \tag{2.12}$$

$$M_2 = f(IR_2) \tag{2.13}$$

$$\alpha = \frac{R_1}{R_2} \tag{2.14}$$

$$M_2 = f\left(\frac{R_1}{\alpha}\right) \tag{2.15}$$

Here we use α to denote the relative spectral intensity between the two objects. Note that R_1 and R_2 are not known, as that presumes knowledge of the illumination spectra. α, however, is known, as the division cancels out influence from the illumination spectra. We do, however, know the following function g:

$$M_1 = f(\alpha f^{-1}(M_2)) \tag{2.16}$$

$$M_1 = g(M_2) \tag{2.17}$$

The goal is then to find $f(x)$ given $g(x)$. We consider the action of f^{-1} on $g(x)$.

$$g(x) = f(\alpha f^{-1}(x)) \tag{2.18}$$

$$f^{-1}(g(x)) = \alpha f^{-1}(x) \tag{2.19}$$

Here we see that f^{-1} is a function that satisfies the above equivalency between different points as defined by the measured $g(x)$. Specifically, I can consider a point (x, y) on f^{-1}. The above relation states that a different point given by $g(x)$ has

output value equal to αy Motivated by this we propose the following algorithm:

$f_0^{-1} = \mathrm{x};$

$\mathrm{n} = 1;$

$\mathrm{t} = 0.01;$

while *not converged* **do**

  $\mathrm{c} = (\alpha\ f_{n-1}^{-1}(\mathrm{x}) + f_{n-1}^{-1}(\mathrm{g(x)}))/2;$

  for *all* x **do**

    $f_n^{-1}(\mathrm{x}) = (1\text{-t})f_{n-1}^{-1}(\mathrm{x}) + \mathrm{t\ c/alpha};$

    $f_n^{-1}(\mathrm{g(x)}) = (1\text{-t})f_{n-1}^{-1}(\mathrm{g(x)}) + \mathrm{t\ c};$

  end

  $f_n^{-1} = \mathrm{smooth}(f_n^{-1});$

  $f_n^{-1} = \mathrm{rescale}(f_n^{-1});$

  $\mathrm{n} = \mathrm{n} + 1;$

end

The main idea is to pick a guess for $f^{-1}(x)$ and then for each point in it find a corresponding point that our equivalency informs us of. We then take an average of the values at each point that are supposed to be equal and reassign the points those values mediated by a relaxation parameter t set empirically to 0.01. $f_n^{-1}(\mathrm{x})$ is internally represented as an array of values mapped to a second array of x values. The function is then put through a rolling average smoothing function in order to ensure that the entirety of the function is updated roughly equally, as in discrete representations certain points may not be operated on equally. Finally, f^{-1} is rescaled so that its max is 1, as the relation specified by g only fixes f^{-1} up to a constant. In practice the relaxation parameter t is increased to 1 as the algorithm converges in order to more strongly enforce the equation and ensure continued convergence as the effective "step" decreases in size. Below are plots of the measured g function, the generated f function and the convergence over time. Here we observe fast convergence to an accurate $f(x)$ as demonstrated by the closeness of the generated $g(x)$ to the measured g. As one would expect, the $f(x)$ reflects a combination of gamma correction and sensor intensity response curves [3].

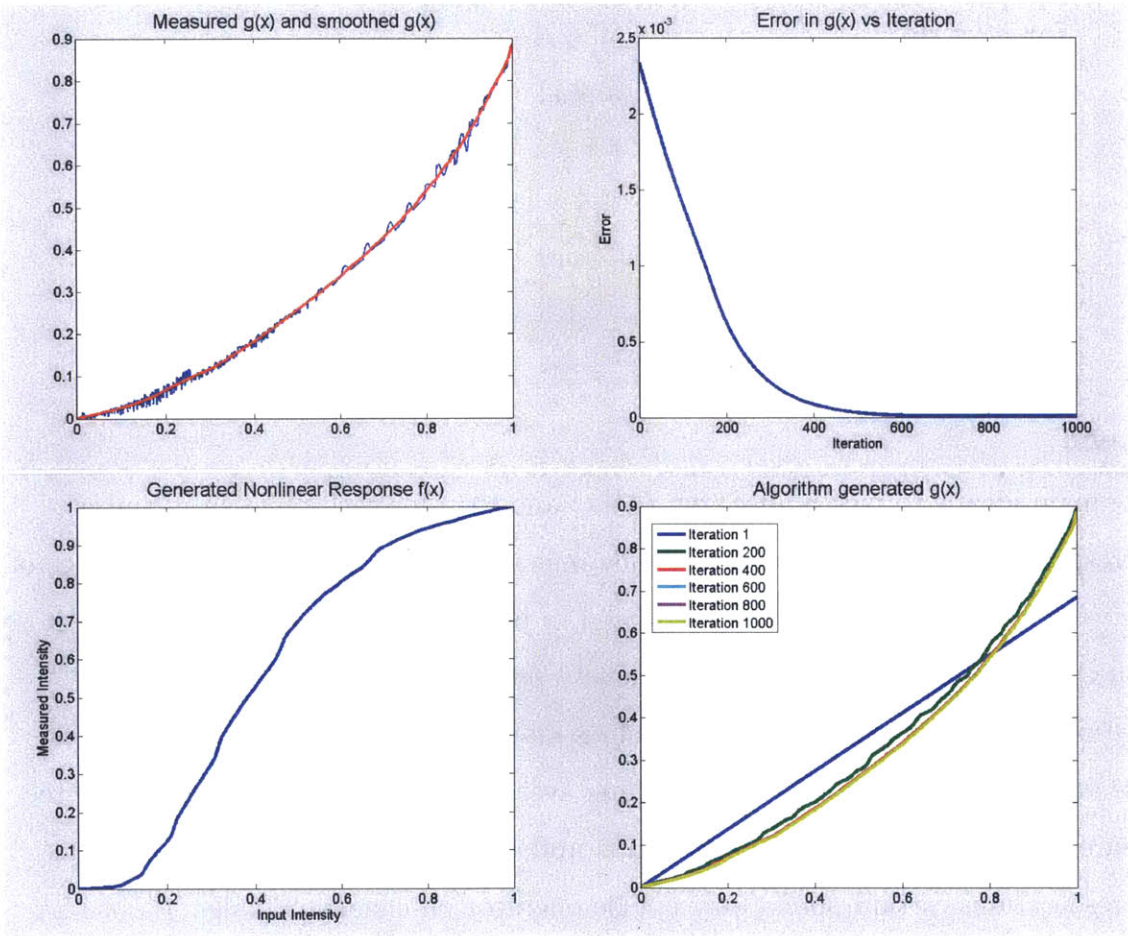

Figure 2-5: Plots of Algorithm Performance and Output

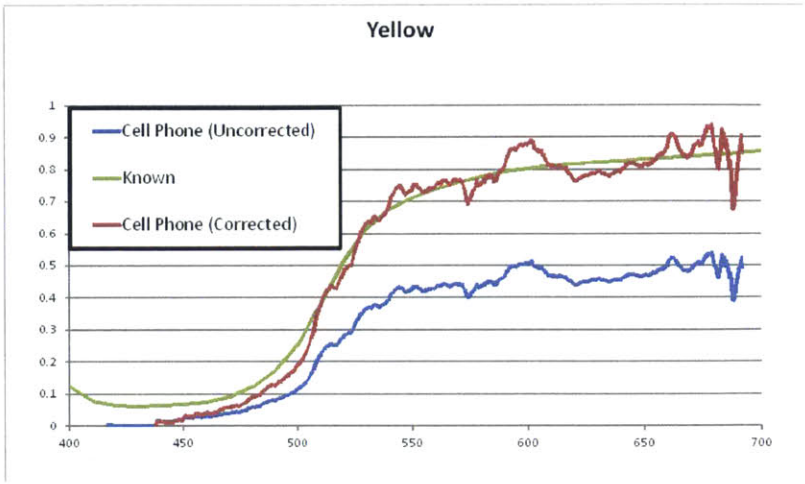

Figure 2-6: Comparison of measured spectra with and without nonlinear correction

Of note is that the final measurement function $g(x)$ appears only slighly nonlinear, but it is generated by a strongly nonlinear sensor response f. This indicates the critical need for this type of detailed solution in correcting the response of the sensor. Figure 2-4 is a comparison between the spectra calculated for the yellow sample on our color chart with and without the nonlinear correction, demonstrating its importance:

2.3.2 Spectral Response Characterization

In order to identify which pixel in an image corresponds to which wavelength it is critical that the spectrometer's spectral response is measured. Typical calibration procedure requires use of a tunable monochromatic light source standard, like a monochromator, or a calibration lamp with a known spectra, such as those commercially available containing noble gases and/or metal vapors. It would be advantageous, however, to enable such a capability without using expensive lab-grade equipment. This requires finding a common, low cost source of a consistent and fine-featured spectra. Previous work has used relatively stable peaks in common compact fluorescent bulbs [6]. There are still a number of variations in the emitted spectra from lamp to lamp, however. For our purposes we used a calibration lamp consisting of Mercury and Argon vapor with known peak structure.

The spectra of this lamp is displayed in Figure 2-5. By fitting a line between the known wavelengths of the peaks and the locations of the peaks on the image sensors it was possible to identify which pixel corresponded to which wavelength. This completes the calibration of the spectrometer.

2.4 Device Performance and Benchmarking

There are two key performance metrics that one would wish to identify when characterizing a spectrometer system. First is the spectral resolution, defined as the minimum distance in wavelength two peaks must be in order to be separately resolved. This can be measured as roughly the width of an infintesimally thin peak. The calibration lamp spectra consists of a series of infintesimally thin peaks, so from this we can determine that our spectral resolution is roughly 5-10 nm over the available bandwidth. The other key metric is noise - that is, what is the natural variation in signal level due to noise on the image sensor as well as quantization noise and JPEG compression artifact (where applicable). In order to measure this we perform a corrected measurement of a flat white sample. This measurement is plotted with the known spectra in Figure 2-9. In principle, the spectra should be uniformly flat. Our data displays an noise RMS of roughly 5% of the total dynamic range, resulting in an ideal SNR of around 5%. This is suitable for many purposes. In cases where spectra are smooth it is further possible to low pass the spectra to suppress noise.

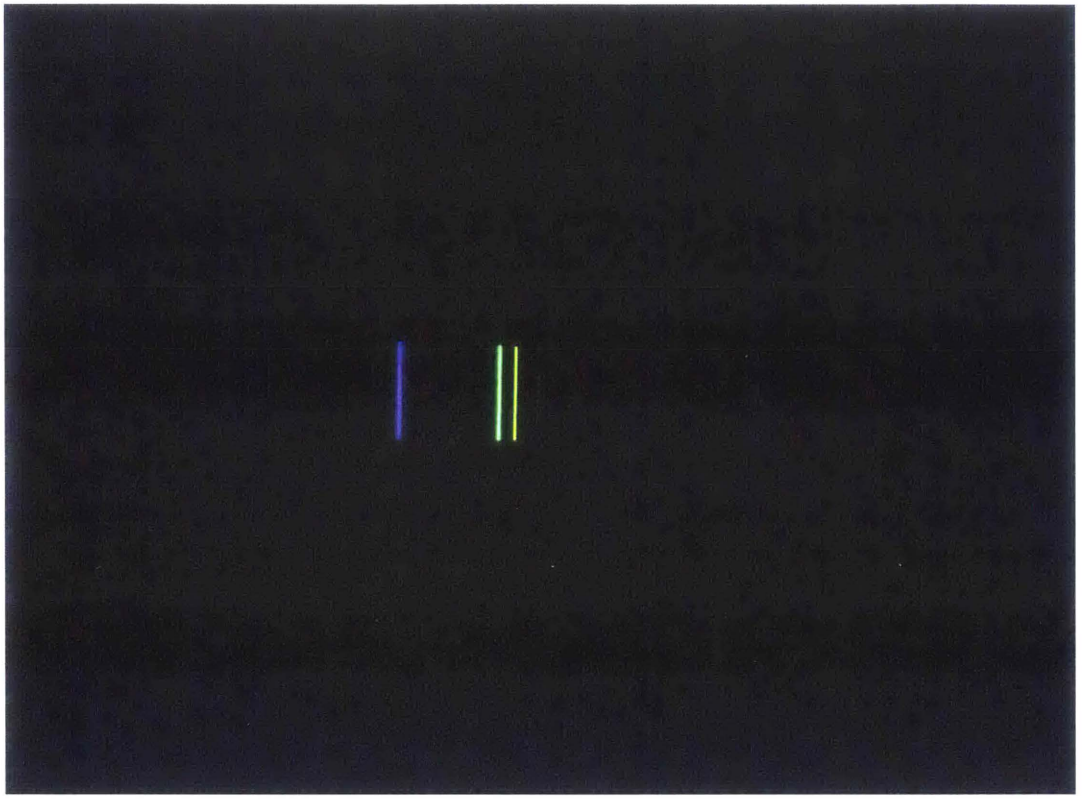

Figure 2-7: Image of calibration lamp through spectrometer

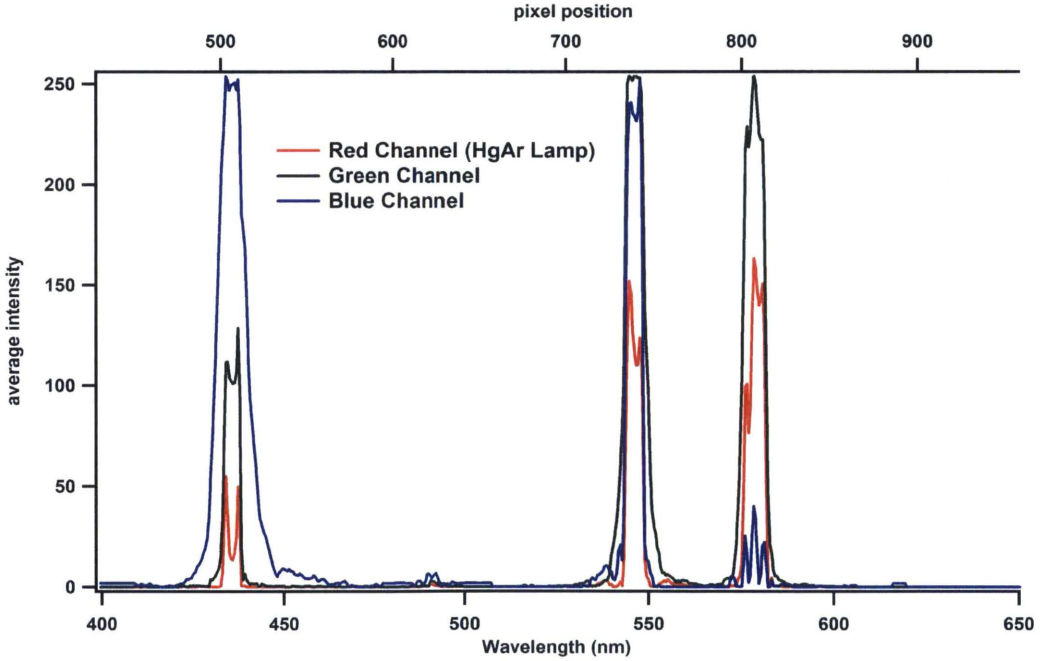

Figure 2-8: Plot of calibration lamp spectra with known spectral peaks

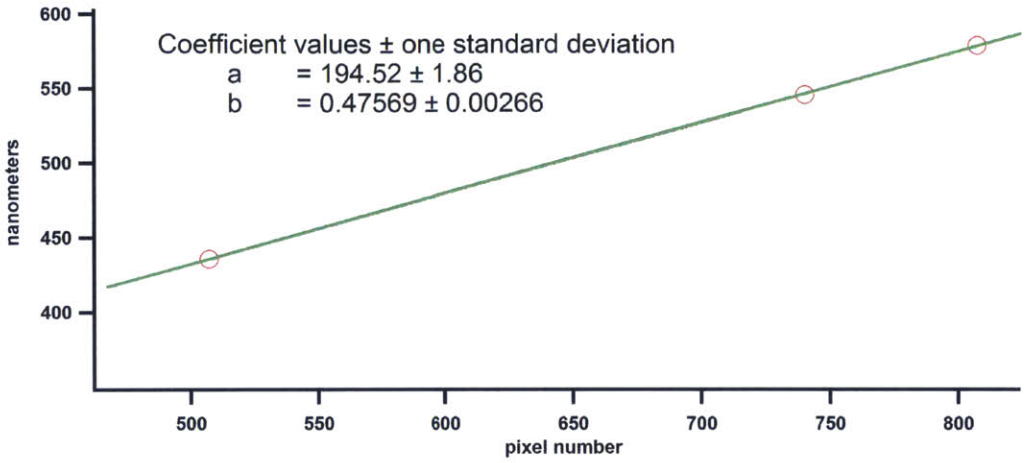

Figure 2-9: Results of fitting peaks to known wavelengths

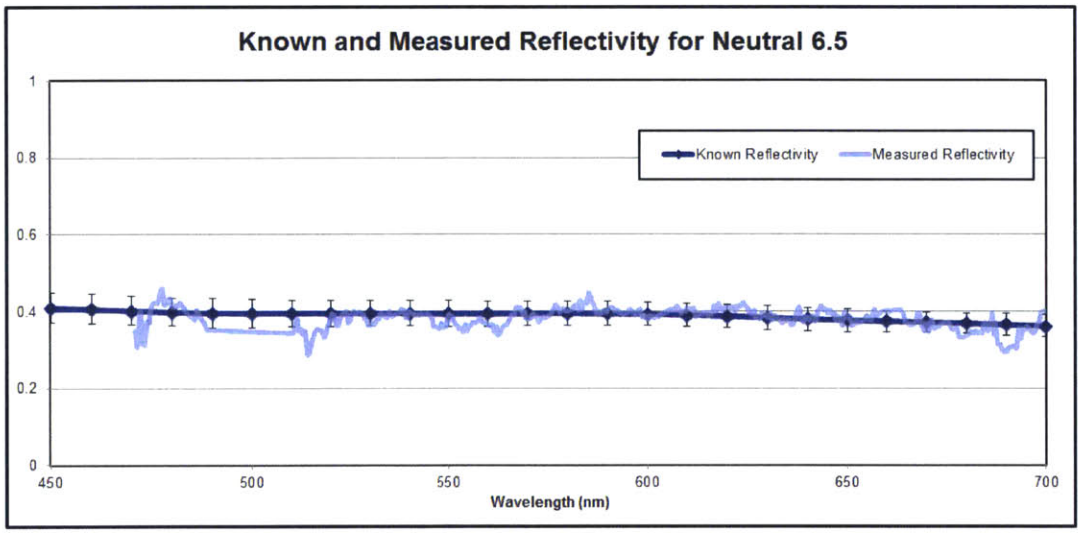

Figure 2-10: Noise performance of cell phone spectrometer

Chapter 3

Mobile Spectral Data Applications

3.1 Colorimetry and Paint Sample Identification

One of the most common applications for spectroscopy is in colorimetry. Colorimetry uses a relatively low-performance spectrometer in order to acquire quantitative information on color. While the human eye is only capable of distinguishing 3 bands of color, full spectral information is required in order to identify an objects color under an arbitrary illumination spectra:

$$I_c = \int d\lambda \; I(\lambda)R(\lambda)C(\lambda) \tag{3.1}$$

Here R denotes the object reflectance spectra, I denotes the illumination spectra and C denotes the spectral response of a given color channel which is typically gaussian shaped. This phenomena explains the observation that two objects appear to be the same color under one lighting condition but can appear to be different colors under a different lighting condition. Since matching colors is a frequent goal in design it is advantageous to measure the reflectance spectra of an object in order to match or mix a color that would match it closely under most lighting conditions. This is directly the measurement that our cell phone spectrometer takes. We then compare those measurements with the manufacturer stated values and those measured by a commericial, off-the-shelf visible spectrometer.

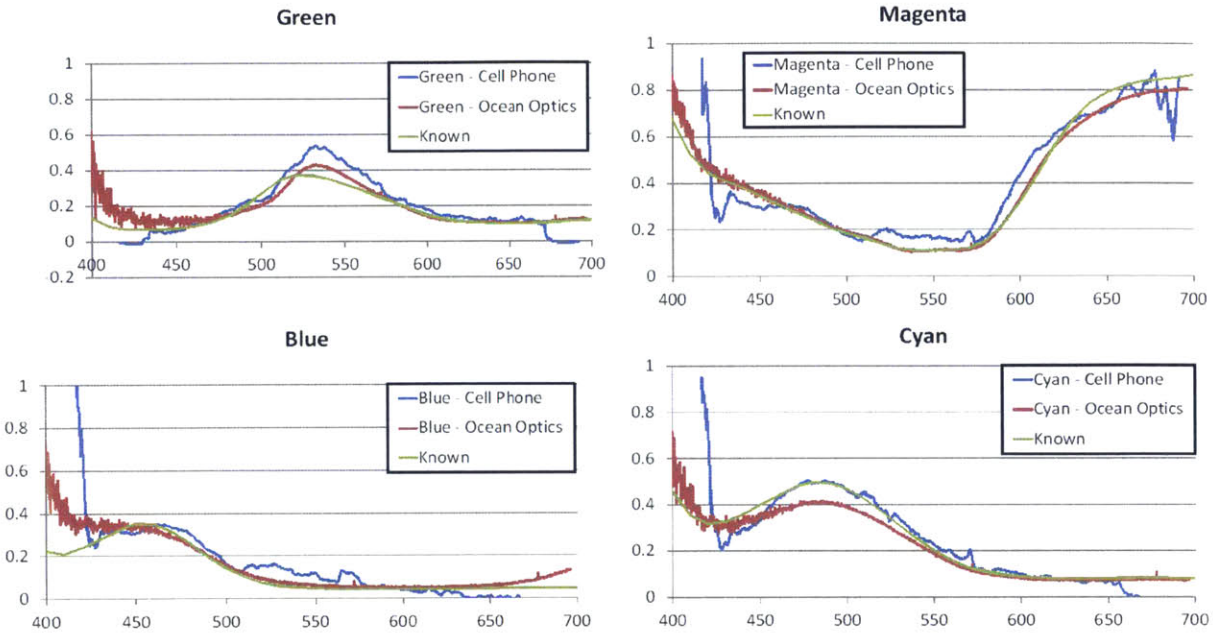

Figure 3-1: Corrected cell phone measurements of colors on standard color chart compared with COTS spectrometer measurements

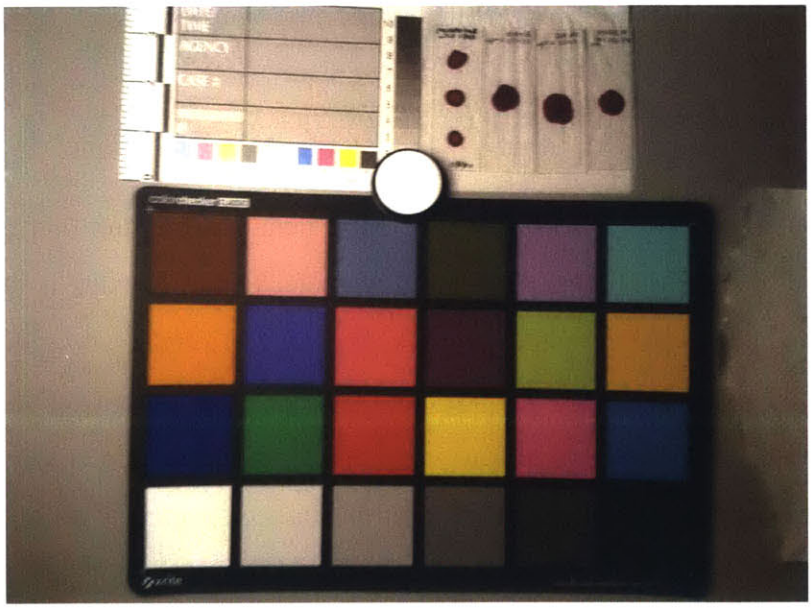

Figure 3-2: Image of standard color chart with blood spots for dating

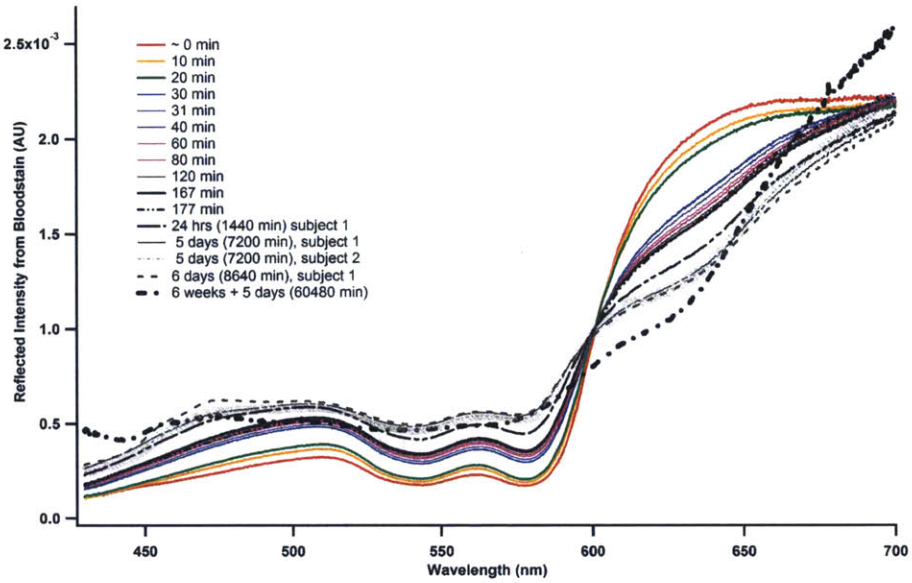

Figure 3-3: Blood spectra measured vs time with Ocean Optics spectrometer

3.2 Blood Spot Dating and Forensic Applications

One primary forensic application for mobile spectrometry is the dating of blood spots. As compounds in blood oxidize after exposure to air the spectra changes in a predictable manner. By measuring the reflectance spectra of a blood spot one can determine the amount of time it has been exposed to the air. This is of direct importance to forensics in the field, as there is often a limit to how many samples can be processed. By determining the age of blood spots it's possible to rule out spots irrelevant to the crime scene and process spots of particular interest.

3.2.1 Algorithms

In order to date unknown blood samples one must construct an algorithm that takes as its input a measured reflectance spectra and as its output produces the time the spot had been exposed. Given that the algorithm is intended to be run on a mobile device, minimizing the computational power required is also of importance. We also seek to construct an algorithm that is robust to changes in substrate and measurement conditions, as well as overall signal intensity. The algorithm achieves these goals by using two spectra depicting fresh and old blood spots. The constant

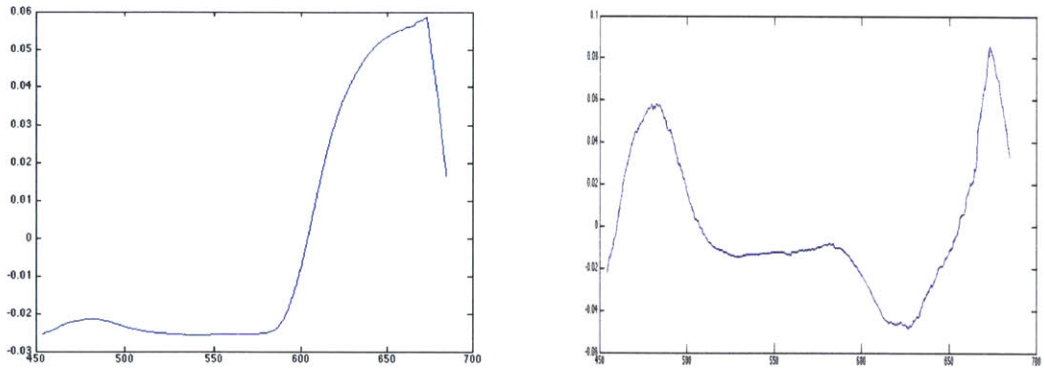

Figure 3-4: Plots of calculated x (left) and y (right) spectra

component of these vectors is removed, and the old blood spectra is orthogonalized with respect to the new blood spectra. The ratio of the dot products of the measured spectra with each of these ideal spectra is calculated, ensuring that the overall intensity of the sample does not affect the algorithm output. This calculated ratio is then compared to a lookup table of ratio values measured in a laboratory. This enables an age to be deduced. The algorithm runs very quickly and provides robust dating results.

$$x = freshSpectra \tag{3.2}$$

$$x = x/|x| \tag{3.3}$$

$$y = oldSpectra - (oldSpectra \cdot freshSpectra)\frac{freshSpectra}{|freshSpectra|^2} \tag{3.4}$$

$$y = y/|y| \tag{3.5}$$

$$value = \frac{measuredSpectra \cdot y}{measuredSpectra \cdot x} \tag{3.6}$$

The motivation for this algorithm is the idea that the blood spectra can be well approximated by a linear combination of the fresh blood spectra and the old blood spectra. The age of the blood can then be determined by considering the relative amplitudes of the those two components. Taking the ratio of the amplitudes makes the algorithm invariant to overall intensity to improve measurement robustness.

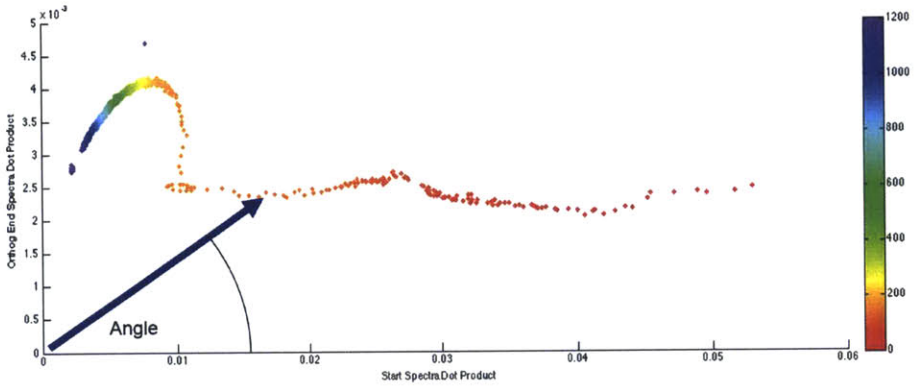

Figure 3-5: Blood spectra dotted with x and y vectors over time in minutes

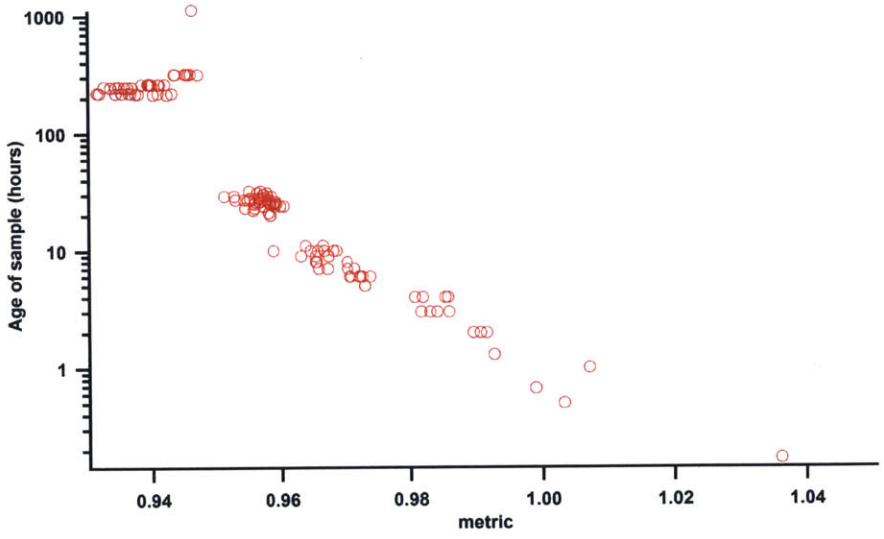

Figure 3-6: Results of aging algorithm over time for a similar algorithm using basis spectra of blood components.

THIS PAGE INTENTIONALLY LEFT MOSTLY BLANK

Chapter 4

Conclusions

An optical system for dispersing light in a spectrometer based on a cell phone camera is designed and optimized. This optical system can be made at low cost for large scale manufacturing, potentially greatly lowering the barrier of entry to a number of interesting and useful measurements. We then designed a novel calibration scheme using a novel algorithm to solve a functional equation describing the nonlinear response of the camera to illumination intensity. This algorithm was used to identify the nonlinear response of the camera and correct measured spectra. The quality of these spectra was measured and quantified. We then applied this portable spectral measurement system to 2 applications of interest, demonstrating the feasibility of using a system like ours for useful commercial applications.
There are a number of areas for further research regarding this research. Preliminary experimentation using rolling shutter effects on phones has suggested the possibility of performing slow time-resolved fluorescence spectroscopy with lifetimes of 1 ms or longer. There's also potential to add a number of other low cost optical elements to the system to extend the range of measurements possible, including polarization and angular dependence. Additionally, UV illumination sources could enable fluorescence spectroscopy for further material identifications. Overall, there is a wide array of measurements that can be made with a low cost system built on a mass-produced cell phone camera. With luck this technology will help lower the barrier of entry to a variety of scientific, medical, and industrial measurements.

THIS PAGE INTENTIONALLY LEFT MOSTLY BLANK

Chapter 5

Appendix

5.1 Supplementary Figures

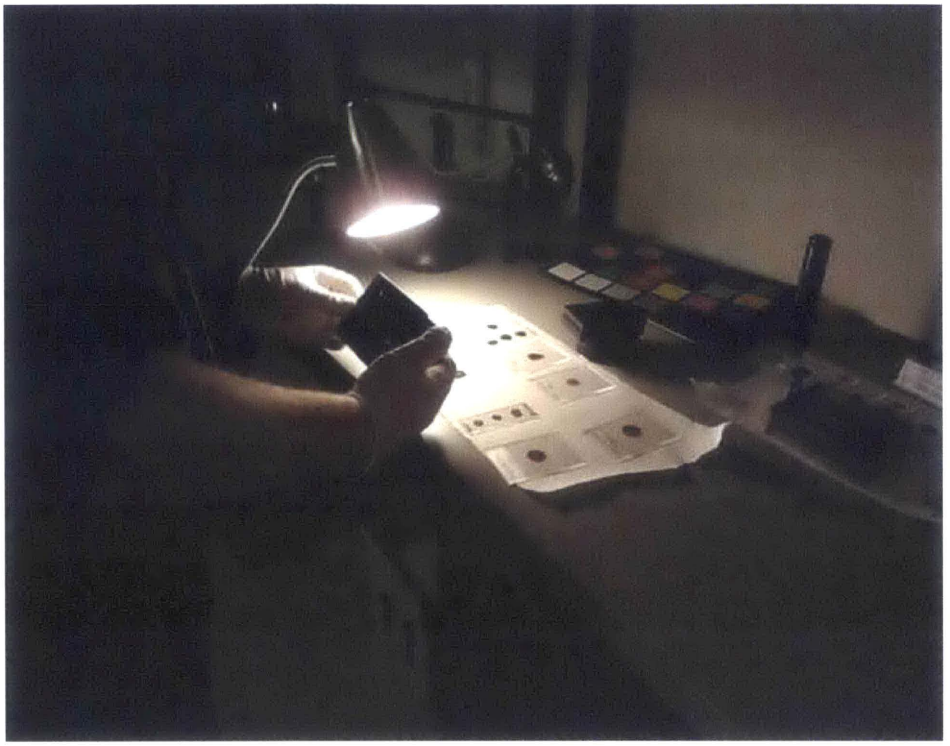

Figure 5-1: Measuring blood samples in the lab with cell phone spectrometer

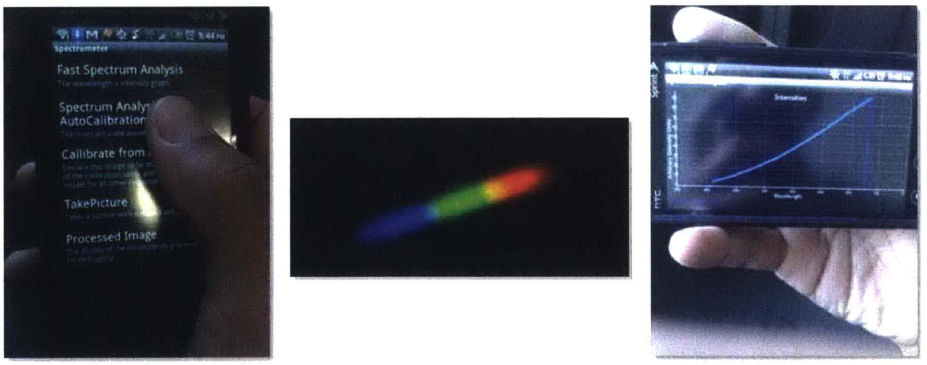

Figure 5-2: Using the cell phone app to measure spectra

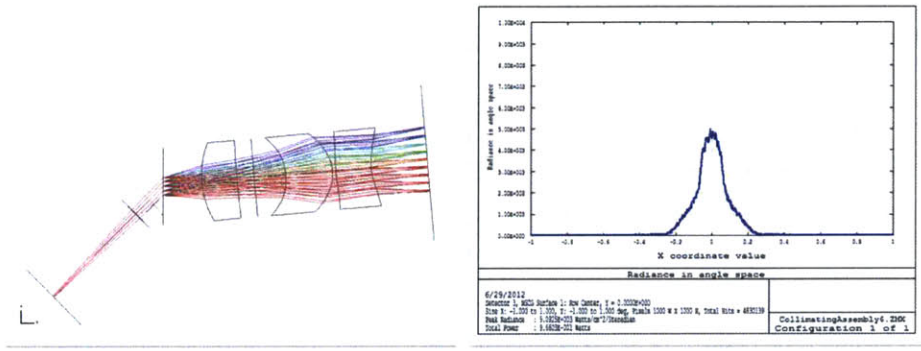

Figure 5-3: Zemax simulations of a spectrometer using patent derived cellphone camera with plot of spot profile

THIS PAGE INTENTIONALLY LEFT MOSTLY BLANK

Bibliography

[1] Dayani Galato, Karina Ckless, Michelle F Susin, Cristiano Giacomelli, Rosa M Ribeiro-do Valle, and Almir Spinelli. Antioxidant capacity of phenolic and related compounds: correlation among electrochemical, visible spectroscopy methods and structure–antioxidant activity. *Redox Report*, 6(4):243–250, 2001.

[2] R Gill, TS Bal, and AC Moffat. The application of derivative uv-visible spectroscopy in forensic toxicology. *Journal of the Forensic Science Society*, 22(2):165–171, 1982.

[3] Michael D Grossberg and Shree K Nayar. Modeling the space of camera response functions. *Pattern Analysis and Machine Intelligence, IEEE Transactions on*, 26(10):1272–1282, 2004.

[4] Public Labs, 2014. [Online; Accessed: 2014-09-01].

[5] Peter Macheroux. Uv-visible spectroscopy as a tool to study flavoproteins. In *Flavoprotein protocols*, pages 1–7. Springer, 1999.

[6] Zachary J Smith, Kaiqin Chu, Alyssa R Espenson, Mehdi Rahimzadeh, Amy Gryshuk, Marco Molinaro, Denis M Dwyre, Stephen Lane, Dennis Matthews, and Sebastian Wachsmann-Hogiu. Cell-phone-based platform for biomedical device development and education applications. *PLoS One*, 6(3):e17150, 2011.

[7] DH Williams, I Fleming, and E Pretsch. Spectroscopic methods. *Organic Chemistry*, (1989), 1989.

[8] Hongying Zhu, Sam Mavandadi, Ahmet F Coskun, Oguzhan Yaglidere, and Aydogan Ozcan. Optofluidic fluorescent imaging cytometry on a cell phone. *Analytical chemistry*, 83(17):6641–6647, 2011.